Title: Infectious disease modeling for public health practice: projections, scenarios, and uncertainty in three phases of outbreak response

Authors: Andrew F. Brouwer[1,2*], Marisa C. Eisenberg[1,2,3], Natalie E. Dean[4,5], Harry Hochheiser[6,7], Philip Huang[8], Joseph R. Coyle,[2,9] Lior Rennert[10,11]

Affiliations:

1. Department of Epidemiology, University of Michigan, Ann Arbor, MI
2. Michigan Public Health Integrated Center for Outbreak Analytics and Modeling, University of Michigan, Ann Arbor, MI
3. Center for the Study of Complex Systems, University of Michigan, Ann Arbor, MI
4. Department of Biostatistics and Bioinformatics, Rollins School of Public Health, Emory University, Atlanta, GA
5. Center for Infectious Disease Modeling and Analytics & Training Hub, Emory University, Atlanta, GA
6. Department of Biomedical Informatics, University of Pittsburgh, Pittsburgh, PA
7. Atlantic Coast Center for Infectious Disease Dynamics and Analytics, University of Pittsburgh, Pittsburgh, PA
8. Dallas County Health and Human Services, Dallas, TX
9. Bureau of Infectious Disease Prevention, Michigan Department of Health and Human Services, Lansing, MI
10. Department of Public Health Sciences, Clemson University, Clemson, SC
11. Center for Public Health Modeling and Response, Clemson University, Clemson, SC, USA

***Corresponding author:** Andrew F. Brouwer, Department of Epidemiology, 1415 Washington Heights, University of Michigan, Ann Arbor, MI; brouweaf@umich.edu

Abstract

Public health departments need evidence-backed projections and scenarios to support decision making in infectious disease outbreaks. However, traditional infectious disease models are often not readily deployable or responsive to the urgent questions and priorities of public health departments or health systems. Moreover, uncertainty in model outputs is frequently misrepresented, undermining trust among public health practitioners and the public. To address these issues, we, the Insight Net Modeling Guidance for Public Health Working Group, used early COVID-19 data from Michigan to illustrate practical and responsive modeling approaches to answer urgent questions in each of three key phases of response to an emerging outbreak: prior to local introduction, early exponential growth, and established transmission with potential interventions. In each phase, we integrate case, hospitalization, and death data and capture ranges of plausible future trajectories. These models, which produce status quo and scenario projections, are intended to inform planning and motivate action rather than forecast precise future outcomes. Importantly, this work offers guidance to focus modeling efforts and provides clear, reproducible examples for how to fit and implement these models, ultimately serving as both a conceptual guide and practical toolkit to support more transparent, timely, and appropriate use of models in outbreak response.

Introduction

The first months of the COVID-19 pandemic were full of uncertainty and a need to act in the face of that uncertainty to protect public health and save lives. State, tribal, local, and territorial (STLT) health departments and healthcare systems needed evidence-backed projections and scenarios to support decision making but had little existing in-house expertise and capacity for infectious disease modeling and analytics (let alone the public health resources, workforce, and information technology infrastructure necessary to respond to a pandemic). New government–academic partnerships arose, often in an *ad hoc* manner, to fill this gap.[1] To improve preparedness for future outbreaks and deepen bonds between health departments and modelers, the Centers for Disease Control and Prevention (CDC) Center for Forecasting and Outbreak Analytics (CFA) was established, along with the National Outbreak Analytics & Disease Modeling Network (Insight Net), a national network of centers comprised of academic, public, and private partners.[2] As members of the Insight Net Modeling Guidance for Public Health Working Group, our team of academic, public health practitioners, and other partners aims to make high-quality models and analytical tools available for outbreak response.

To best use infectious disease models for outbreak response, we need to distinguish between *forecasting*—the prediction of what cases, hospitalizations, and deaths will be in the future—and *scenario modeling*—the projection of these quantities under the status quo and a range of assumptions. Mechanistic infectious disease models are notoriously poor at forecasting, as real-world situations typically quickly deviate from the status quo assumptions of these models.[3] However, infectious disease models excel at scenario modeling, which can be thought of as *in silico* experiments to answer questions like, "*how bad might outcomes get if we do not intervene?*", "*are we likely to exceed hospital capacity?*", and "*how could a given intervention change future trajectories?*" This ability to design, evaluate, and compare counterfactual scenarios ("what would have happened if…") is a particular strength of infectious disease models, as is their ability to retrospectively evaluate the impact of public health interventions. In this article, we focus on scenario modeling, building status quo scenarios based on recent data and illustrating some alternative scenarios.

This article is intended for STLT public health department and healthcare system epidemiologists and their academic or private partners assisting with modeling during an infectious disease outbreak. We illustrate—with accompanying open code—practical and responsive modeling approaches suited to answering urgent questions in each of three key phases of an emerging outbreak: prior to local introduction, early exponential growth, and

established transmission with potential interventions. Beyond providing a starting point to avoid the need to “reinvent the wheel” for each new outbreak, this work aims to ensure that model outputs are both interpretable and actionable by public health practitioners. Importantly, we emphasize that models do not need to be complicated to be useful: often a relatively simple, “back-of-the-envelope” analytic approach is sufficient in many cases. Our approach also pays careful attention to the inclusion of uncertainty in projections; our goal is to balance the need to take “the number” to decision makers with the need to accurately convey how much confidence there is in that number, even if that’s just “best case, worse case”. It is very easy to misrepresent uncertainty in the future trajectories projected by infectious disease models, reducing both public health partners’ and the public’s confidence in models. By establishing a shared framework, we seek to support more effective, transparent, and responsible use of models in outbreak situational awareness and response.

Methods

Overview

Below, we outline three phases of outbreak response that inform our case studies, discuss the data we use to inform our models, describe exponential growth and infectious disease transmission models to project infections, reported cases, hospitalizations, and deaths, and illustrate how we quantify uncertainty in model projections. Many technical details are reserved for the Technical Supplement, and all data and code are available in a public repository (see Data Availability). Deidentified, aggregated data for public health surveillance were provided by the Michigan Department of Health and Human Services, and this study was not regulated as human subjects research (University of Michigan Health Sciences and Behavioral Sciences Institutional Review Board HUM00181319).

Three phases of outbreak response

Data availability and the modeling needs of STLT health departments and healthcare systems change across different phases of outbreak response. Broadly, our goal is to project and quantify uncertainty in reported cases, hospitalizations, and deaths under status quo scenarios. Our models can be extended as needed to include other measures of interest specific to a partner’s needs, such as personal protective equipment (PPE), hospital bed capacity, and staffing.

Phase 1: Preliminary projections before local spread. Before an expected outbreak has been detected locally, STLT health departments can use models to understand the potential speed and magnitude of local spread, supporting advanced planning, requests for funding or supplies, and communication with stakeholders. In this phase, exponential growth models adequately capture potential spread. Our models provide preliminary projections based on information from historical or ongoing outbreaks.

Phase 2: Local exponential growth. Once local transmission has been sustained for several weeks and the epidemic is growing exponentially, STLTs health departments need local, short-term status quo projections. Our models provide short-term exponential projections with parameters informed by recent, local data.

Phase 3: Established transmission with potential interventions. If the outbreak continues to spread, STLT health departments need to consider and evaluate a variety of possible interventions and scenarios to better guide their decision making. Mechanistic infectious disease models are well-suited both to capturing realistic dynamics and uncertainty in status quo projections and projecting alternative scenarios of interest.

Infectious disease data streams

We rarely have information about the underlying burden of infection. Instead, the data available for modeling is primarily in the form of lists of reported cases—typically those individuals who were symptomatic and sought testing or medical care. These “line lists” are often simplified to numbers of cases per date. As discussed in the Technical Supplement, we recommend using symptom onset date to capture the infectious disease dynamics. We drop data for recent onset dates (“burn-in”) because recent data are incomplete due to reporting lags (Figure 1A). In addition to case data, hospitalizations and deaths are also frequently reported and projected in outbreaks.

Our models use six data parameters that describe the relationships between cases, hospitalizations, and deaths: the fraction of infections reported as cases (infection–case ratio) φ_{IC}, the fraction of cases who become hospitalized (case–hospitalization ratio) φ_{CH}, the fraction of cases who die (case–fatality ratio) φ_{CD}, the case reporting lag τ_{IC}, the lag between case reporting and hospitalization τ_{CH}, and the lag between case reporting and death τ_{CD} (Figure 1B; Table 1). The infection–case ratio cannot be determined from case data alone, so a range of realistic values informed by historic outbreaks is typically considered. A reasonable range for the case reporting lag can be set from historic outbreaks or from the estimated incubation period

and the mean difference between symptom onset and reporting date in the surveillance system. The remaining parameters can be estimated by comparisons of the data streams or, in Phases 2 and 3, through fitting the model to the data. Reporting delays are often exacerbated by high cases numbers that exceed public health workforce capacity.

Exponential growth model

In Phases 1 and 2, when case numbers approximately follow exponential growth, we will use an *exponential growth model*. This class of model should be thought of as informed back-of-the-envelope calculations for generating short-term, status quo scenario projections, as real, longer-term dynamics will deviate from these models.

We model numbers of actual infections $Y(t)$, reported cases $C(t)$, hospitalizations $H(t)$, and deaths $D(t)$ as functions of time since outbreak start t. In addition to the data parameters described above, these models are informed by the initial number of cases $C(0)$ and the epidemic doubling time t_d (Table 1).

$$\begin{aligned} Y(t) &= C(0) \times 2^{\frac{t+\tau_{IC}}{t_d}} / \varphi_{IC}, \\ C(t) &= C(0) \times 2^{\frac{t}{t_d}}, \\ H(t) &= C(0) \times 2^{\frac{t-\tau_{CH}}{t_d}} \times \varphi_{CH}, \\ D(t) &= C(0) \times 2^{\frac{t-\tau_{CD}}{t_d}} \times \varphi_{CD}. \end{aligned} \quad \#(1)$$

The model in Eqs (1), which captures exponential growth in cases and the delays and ratios between the data streams, is used to project $Y(t)$, $C(t)$, $H(t)$, and $D(t)$ for each day t.

Infectious disease transmission model

In Phase 3, we use a compartmental *infectious disease transmission model*, based on a susceptible–latent–infectious–recovered (SLIR) framework and simulated with differential equations.[4–6] The model describes the fraction of the population in each compartment (Figure 2), accounting for the transmission rate (β), the rate of transition from the latent to infectious phase (σ), and the recovery rate from the infectious compartment (γ). The basic reproduction number R_0—the number of secondary cases generated by a single infectious individual in an otherwise susceptible population—here equal to β/γ, is more intuitive than the transmission rate: we recommend reporting R_0 rather than β when communicating with public health partners or the public. The system of differential equations for the model is given in Eqs (2). As discussed

in more detail in the Technical Supplement, to more realistically model the durations of the latent and infectious periods, we model each as of them as two consecutive compartments.[7]

$$
\begin{aligned}
{dS}/{dt} &= -\beta S(I_1 + I_2), \\
{dL_1}/{dt} &= \beta S(I_1 + I_2) - 2\sigma L_1, \\
{dL_2}/{dt} &= 2\sigma(L_1 - L_2), \\
{dI_1}/{dt} &= 2\sigma L_2 - 2\gamma I_1, \\
{dI_2}/{dt} &= 2\gamma(I_1 - I_2), \\
{dR}/{dt} &= 2\gamma I_2.
\end{aligned}
\qquad \#(2)
$$

The model initial conditions are described in the Technical Supplement, as a function of the fraction of individuals that are initially infectious, I_0.

To connect the model to data and generate projections for numbers of actual infections $Y(t)$, reported cases $C(t)$, hospitalizations $H(t)$, and deaths $D(t)$ over time t, we again account for the data delay and ratio parameters. Additionally, we need the size of the at-risk population κ (not the catchment population, which may include a substantial recovered fraction or otherwise not be at risk of infection in the short-term) to translate the simulated *fraction* infectious into *numbers* of infectious individuals. Importantly, the values of the size of the at-risk population κ and the infection–case ratio φ_{IC} cannot be separately determined from case data. The observed case trajectory could be explained equally well by a larger at-risk population paired with a smaller infection–case ratio or by a smaller at-risk population paired with a larger infection–case ratio. There would be more unreported cases in the first situation, but without other data, e.g., serosurveys, we cannot determine which situation is correct. To address this issue, $\kappa\varphi_{IC}$ is treated as a single, estimated parameter. For brevity, the technical details describing the connection between the Eqs (2) and $Y(t)$, $C(t)$, $H(t)$, and $D(t)$ are given in the Technical Supplement.

Fitting models to data

In Phases 2 and 3, we fit models to local data using parameter estimation. We assume that daily reported cases, hospitalizations, and deaths are drawn from Poisson distributions with means $C(t)$, $H(t)$, and $D(t)$, respectively. The negative log likelihood $NLL_C(\theta)$ of observing the reported cases $z_C(t)$ on each day t in the $\{t_C\}$, the set of days included for fitting cases, is given in Eq (3). In lay terms, this equation measures the discrepancy between the modeled cases

$C(t)$ and the observed cases $z_C(t)$, so that we can minimize that discrepancy by adjusting the parameters θ.

$$NLL_C(\theta) = \sum_{t \in \{t_C\}} C(t;\theta) + \sum_{t \in \{t_C\}} z_C(t)! + \sum_{t \in \{t_C\}} z_C(t) \times \log\big(C(t;\theta)\big) \#(3)$$

The negative log-likelihoods for hospitalizations and deaths are defined analogously, using hospitalization and death data, $z_H(t)$ and $z_D(t)$, and their data periods $\{t_H\}$ and $\{t_D\}$, respectively. Further details are given in the Technical Supplement. The total negative log-likelihood is the sum of the three negative log-likelihoods: $NLL(\theta) = NLL_C(\theta) + NLL_H(\theta) + NLL_D(\theta)$. We find the best fit parameters θ by minimizing the negative log-likelihood $NLL(\theta)$. In our case studies, below, we use the `optim` function in R v4.4 with the Nelder-Mead algorithm, a classic and widely used parameter estimation approach.

The importance of quantifying and communicating uncertainty

Although decision makers often like the simplicity of a single number (e.g., the best-fit prediction), it is best to provide an estimate of the degree of uncertainty in that number. Indeed, inappropriately confident predictions can reduce trust in models and modelers, as was highlighted in the sensational overestimates given in the 2014–15 Ebola outbreak[8,9] and more recently in the COVID-19 pandemic.[10] Even relatively crude approaches to uncertainty, giving "best" and "worst" case scenarios can be extremely helpful in providing intuition to decision makers. We want to be able to ask questions like, "*What range of dynamics is possible between the best and worst cases?*" and, "*Is substantial action needed to avoid even the best-case scenario?*"

There are several sources of uncertainty in outbreak analytics and modeling. One source is noise in the data itself. Another source comes from not knowing the current, underlying state of the system (e.g., the actual number of infected individuals) or the values of model parameters (e.g., the reproduction number or case reporting fraction). A state in the model is *observable* if it can be determined from the available data. In an infectious disease outbreak, the numbers of reported cases, hospitalizations, and deaths are observable, but the number of infections is typically not. A model parameter is *identifiable* from the data if there is a unique, best-fit value of that parameter associated with the data. For example, the case–fatality ratio is typically identifiable (as we observe both cases and deaths), but the infection–case ratio and the case reporting lag will not be (as we do not observe infections). There is a rich literature on

identifiability and observability of parametric models,[11–14] and we are only scratching the surface here.

In an outbreak—and particularly during the growth phase of an outbreak—many relevant parameters will not be identifiable from the available data. However, projections may depend on the specific values of unidentifiable parameters values or unobservable states, and so we need to rely on external information, such as estimates from other outbreaks, similar pathogens, or even just "reasonable" ranges determined by the modeler or other expert opinion.

There are many approaches to uncertainty analysis, and we will use a different approach in each of the three Phases of the outbreak. In Phase 1, there is no local data, and our uncertainty will be based only on reasonable ranges of the parameters. Using Sobol' sampling,[15] we sample 10,000 combinations of parameters from across their ranges, generate projections for each combination, and calculate credible intervals for each day in the projection.

In Phase 2, we use reasonable ranges for the parameters that are not identifiable, and we will create reasonable ranges for the identifiable parameters consistent with the noise in the data. For this case study, we will use +/- 25% of the best-fit parameter values, but a larger range may be appropriate for capturing noisier data. As in Phase 1, we sample 10,000 combinations of parameters from across their ranges, generate projections for each combination, and calculate quantiles for each day in the projection

The mechanistic model in Phase 3 has a larger number of unidentifiable parameters that cannot be uniquely estimated from the data but can affect the projection trajectory. To overcome this difficulty, we will use a two-step combination of estimation and sampling. The general idea is that we generate a large number of combinations of reasonable values for the unidentifiable parameters in the first step (Figure 3A), and then for each of these combinations, we estimate the identifiable parameters using maximum likelihood estimation as discussed in the previous section (Figure 3B).[16] To ensure that each of these parameter sets reasonably fits the data, we drop parameter sets whose NLLs exceed our rule of thumb of 110% of the minimum NLL. We then generate a projection for each of the remaining parameter combinations (Figure 3C) and plot the bounds for the 50% and 95% credible intervals (Figure 3D), indicating a region of "more likely" projections and the range of "best" and "worst" case projections. (Figure 3C and D also represent how uncertainty is estimated for Phases 1 and 2). In the Phase 3 case study, we use only 500 samples because of the computational burden, but more would be better if time allows.

Case studies

We illustrate our modeling approaches in each of the three Phases using COVID-19 case, hospitalization (new confirmed and probable COVID-19 admissions), and death data from Michigan, 2020–21.

Phase 1: Preliminary projections before local spread

Approach. The modeling goal of Phase 1 is to understand the potential speed and magnitude of local spread, supporting advanced planning and communication with stakeholders. To illustrate the Phase 1 approach, we use the best-guess parameter values and ranges in Table 1, starting from a single infected individual, and provide six-week projections.

*Results. S*ix weeks after introduction, we project 4,100 (50% CI: 2,400–7,800; 95%CI: 1,500–15,100) daily reported cases; 54,000 (50% CI: 33,000–154,000; 95%CI: 12,000–653,000) daily actual infections; 120 (50% CI: 60–190; 95%CI: 20–550) daily hospitalizations, and 6 (50% CI: 3–11; 95%CI: 1–33) daily deaths (Figure 4).

Phase 2: Local exponential growth

Approach. The modeling goal of Phase 2, once local circulation has begun, is to provide short-term projections to guide planning. To illustrate the Phase 2 approach, we fit our exponential models to the four weeks of data preceding November 1, 2020 (chosen as a typical example of epidemic growth when all data streams were available), using a 1-week burn-in for the case data, and make a two-week status-quo projection. In this phase, projections beyond 2-weeks are generally unreliable because of how quickly real dynamics can change and deviate from exponential models. As summarized in Table 1, we fix τ_{CH} and τ_{CD} to data-driven values and only estimate the initial case counts, doubling time, case–hospitalization ratio, and case–fatality ratio (C_0 ,t_d, φ_{CH}, and φ_{CD}). Note that the infection–case ratio and delay (φ_{IC}, τ_{IC}) are not identifiable from the available data, so we use the best-guess estimates and ranges from Phase 1 to estimate infections (included in the supplemental code but not shown in the results).

Results. Two weeks after November 1, we project there would be 6,600 (50%CI: 5,400–8,300; 95%CI: 4,100–12,000) reported cases, 400 (50%CI: 330–5000; 95%CI: 230–740) daily hospital admissions, and 60 (50%CI: 50–73; 95%CI: 37–100) deaths (Figure 5).

Phase 3: Established transmission with potential interventions

Approach. The modeling goal of Phase 3 is to make projections accounting for dynamics other than exponential growth and to evaluate potential interventions and scenarios. To illustrate the Phase 3 approach, we fit our models to the six weeks of data preceding April 5, 2021 (chosen

as a nice example of how scenario models can be revisited in hindsight) and make four-week status-quo projections. As summarized in Table 1, parameters τ_{CH} and τ_{CD} are fixed to values, as in Phase 2. The latency (σ) and recovery rate (γ) parameters and case reporting delay τ_{IC} are sampled from ranges. The initial fraction infectious, I_0, is not observable, and we sample it from a large range of possible values (1E-6, 1E-2). For given set of fixed and sampled parameters, we estimate identifiable parameter combinations β, $\kappa\varphi_{IC}$, φ_{CH}, and φ_{CD}.

We illustrate alternative scenario modeling by simulating a ±25% change to the transmission rates starting on April 5. It may be useful to generally prepare status quo scenarios and scenarios with potential changes in the transmission rate to capture some additional uncertainty in projection caused by time-varying parameters. Scenarios can also be used to estimate the potential impact of larger changes, such as stay-home orders or social distancing fatigue. Scenario projections can also be revisited weeks later, to see how consistent actual dynamics were with each of the scenarios considered. Here, we compare the data as eventually reported to a scenario with a 45% transmission rate reduction.

Results. Four weeks after April 5, 2021, we estimate there would be a median 14,200 (50%CI: 9,400–21,000; 95%CI: 4,600–30,700) reported cases, 1,010 (95%CI: 750–1,350; 95%CI: 430–1,750) daily hospital admissions, and 125 (50%CI: 104–147; 95%CI: 73–169) deaths (Figure 6A–C). A wide range of future trajectories—from continued explosive growth to susceptible burnout and epidemic decay—is consistent with the recent epidemic growth trajectory, highlighting the difficulty of epidemic forecasting given the data that are typically available.

Under the scenario with a 25% increase in transmission, we project a median 21,900 reported cases, 1,540 daily hospital admissions, and 169 deaths, and, under the scenario with a 25% decrease in transmission, we estimate a median 7,400 reported cases, 580 daily hospital admissions, and 86 deaths (Figure 6D–F). In retrospect, the scenario with a 45% decrease in the transmission rate is consistent with the cases, hospitalizations, and deaths as they were eventually reported (Figure 6G–I).

Discussion

We developed models to project infections, cases, hospitalizations, and deaths, along with robust uncertainty estimates, under status quo assumptions in three phases of outbreak response: before local transmission, local exponential growth, and established transmission with potential interventions. These projections are not forecasts and are not likely to come to pass as is. Instead, they provide information about the potential magnitude of the problem if nothing

changes. And change is likely: either through action coordinated by STLT health departments or simply as a function of behavior change by the public in response to news. Our projections provide a benchmark for decisions makers to determine if and what action to take, such as planning for hospital capacity, applying for aid for additional protective equipment, starting early surveillance to catch silent circulation prior to hospitalizations or deaths, and building support for larger interventions (e.g., health campaigns, vaccination clinics, or stay-at-home orders).

As we see here, even relatively simple analytic approaches (exponential models) can be useful for public health practitioners if thoughtfully applied. Our models are intentionally simple, generic, and flexible enough to fit many outbreaks; they are starting points that can (and will likely need to) be modified, adapted, and tuned to specific outbreaks. These models are not intended as a theoretical exercise; they need to be responsive to the specific needs of STLT public health departments and healthcare systems. To be responsive, modelers may need to add projections of other quantities of interest; for the COVID pandemic, these projections could have included intensive care unit beds, PPE needs, or extracorporeal membrane oxygenation (ECMO) machines. Public health partners may also be interested in projections by geographic area (e.g., county), age group, race and ethnicity group, or other subgroups of interest. Ultimately, modelers need to be in close conversation with public health partners, not only to deliver responsive modeling but also to effectively and accurately communicate those estimates and their uncertainties.

We again emphasize that these model projections should not be thought of as forecasts, meaning that they are not projecting cases, hospitalization, and deaths as we expect them to be. Deviation from the projections does *not* mean that the models were “wrong.” Instead, reality may be deviating from the status quo assumptions of the model, particularly through time-varying parameters (e.g., changing transmission rate or case–fatality ratio, etc). Rather than treating the status quo model projections as forecasts, modelers can provide projections from a range of possible scenarios (Figure 6D–F). It is then possible to see, in retrospect, which scenario was most consistent with what occurred (Figure 6G–I). One challenging aspect of providing these modeling projections that we did not discuss in detail is how to make serial projections while underlying parameters change, e.g., as interventions are implemented or as the public’s behavior changes. One could incorporate changing dynamics into the model directly, possibly informed by previous scenario modeling. For example, in Figure 6G–I, we might take the 45% transmission rate reduction scenario as the new status quo from which to

make subsequent status-quo and scenario projections. Alternatively, parameters can themselves be modeled as time-varying, as step functions, splines, or other functional forms.

Our approach to uncertainty encourages modelers and public health partners to avoid overconfidence in best-fit projections because those projections are based on assumptions that we should not have confidence in. There are multiple combinations of unknown parameters, the population at risk, and fraction of the population that is infectious that are consistent with recently observed data (Figure 5A–C). It is also important to communicate with public health partners or to the public that the uncertainty bounds are for status quo scenarios and do not include the possibility of changes in transmission or other parameters and that they do not represent forecasts; pairing the status quo scenario projections with alternative scenario projections can help to make this distinction clear.

In our collective experience as part of Insight Net and as academic modelers or public health professionals, we recognize that STLT public health departments and healthcare systems rarely need complex modeling techniques, especially in the early days of an outbreak. Instead, educated guesses and “back-of-the-envelop” calculations can be more effective when they are fast and responsive and easy to communicate. Here we have provided modeling approaches, with associated open code, to serve as what we hope to be an accessible starting point for a wide variety of both academic and public health users.

Acknowledgments

We thank Juliet Pulliam for her contributions to the early discussions of this work, which helped shape the case studies. We thank the members of the Insight Net Modeling Guidance for Public Health Working Group for providing critical feedback. We thank Annie Niu, Troy Zhou, and Stephanie Iorga for reviewing and testing the code.

Declaration of competing interests

All authors declare that they have no competing interests.

Study Funding

This publication was made possible by the Insight Net cooperative agreements NU38FT000001, NU38FT000002, NU38FT000004, and NU38FT000011 from the CDC's Center for Forecasting and Outbreak Analytics (CDC-RFA-FT-23-0069). Its contents are solely the responsibility of the authors and do not necessarily represent the official views of the Centers for Disease Control and Prevention. LR also reports funding from National Institutes of Health (NIH) National Library of Medicine (NLM) award R01LM014193.

Data Availability

All data and code have been made available in a Zenodo repository at https://doi.org/10.5281/zenodo.17253532.

References

1. León TM, White LA, Spindler H, et al. Fostering public health and academic partnerships during and beyond a public health emergency: lessons learned from COVID-19. *Am J Epidemiol* 2025; 194: 1482–1484.

2. Centers for Disease Control and Prevention (CDC). Insight Net.

3. Metcalf CJE, Lessler J. Opportunities and challenges in modeling emerging infectious diseases. *Science* 2017; 357: 149–152.

4. Anderson RM, May RM. *Infectious Diseases of Humans: Dynamics and Control*. Oxford: Oxford University Press, 1992.

5. Diekmann O, Heesterbeek J. *Mathematical Epidemiology of Infectious Diseases: Model Building, Analysis, and Interpretation.* Hoboken, NJ: Wiley, 2000.

6. Hethcote HWH. The mathematics of infectious diseases. *SIAM Rev* 2000; 42: 599–653.

7. Hurtado PJ, Kirosingh AS. Generalizations of the 'Linear Chain Trick': incorporating more flexible dwell time distributions into mean field ODE models. *J Math Biol* 2019; 79: 1831–1883.

8. Chowell G, Viboud C, Simonsen L, et al. Perspectives on model forecasts of the 2014–2015 Ebola epidemic in West Africa: lessons and the way forward. *BMC Med* 2017; 15: 42.

9. Carias C, O'Hagan JJ, Gambhir M, et al. Forecasting the 2014 West African Ebola Outbreak. *Epidemiol Rev* 2019; 41: 34–50.

10. James LP, Salomon JA, Buckee CO, et al. The Use and Misuse of Mathematical Modeling for Infectious Disease Policymaking: Lessons for the COVID-19 Pandemic. *Med Decis Making* 2021; 41: 379–385.

11. Cobelli C, DiStefano JJ. Parameter and structural identifiability concepts and ambiguities: a critical review and analysis. *Am J Physiol* 1980; 239: R7-24.

12. Jacquez JA. Identifiability and parameter estimation. *JPEN J Parenter Enteral Nutr* 1991; 15: 55S--59S.

13. Villaverde AF. Observability and Structural Identifiability of Nonlinear Biological Systems. *Complexity* 2019; 2019: 8497093.

14. Miao H, Xia X, Perelson AS, et al. On Identifiability of Nonlinear ODE Models and Applications in Viral Dynamics. *SIAM Rev* 2011; 53: 3–39.

15. Sobol' IM. On the distribution of points in a cube and the approximate evaluation of integrals. *USSR Comput Math Math Phys* 1967; 7: 86–112.

16. Brouwer AF, Eisenberg MC, Bakker KM, et al. Leveraging infectious disease models to interpret randomized controlled trials: Controlling enteric pathogen transmission through water, sanitation, and hygiene interventions. *PLOS Comput Biol* 2022; 18: e1010748.

Tables

Table 1: Summary of model parameters for COVID-19 in Michigan 2020–21 in each case study across the three outbreak response phases. In Phase 1, we use a best-guess and range for each parameter (with values derived from the literature or expert opinion). In Phases 2 and 3, we fix some data-driven parameters, sample others from a range, and estimate the remaining parameters.

		Case Studies		
Parameter	Description	Phase 1	Phase 2	Phase 3
Data parameters (both models)				
φ_{IC}	Infection–case ratio	0.25 (0.05–0.50)	0.25 (0.05–0.50)	Estimated as $\kappa\varphi_{IC}$
φ_{CH}	Case–hospitalization ratio	0.10 (0.02–0.20)	Estimated	Estimated
φ_{CD}	Case–fatality ratio	0.03 (0.01–0.05)	Estimated	Estimated
τ_{IC}	Case reporting delay (days)	6 (4–10)	6 (4–10)	6 (4–10)
τ_{CH}	Hospitalization delay (days)	6 (4–10)	6	6
τ_{CD}	Death delay (days)	15 (10–20)	15	15
Exponential growth model parameters				
$C(0)$	Initial number of cases	$\varphi_{IC} \times 2^{\tau_{IC}/t_d}$	Estimated	—
t_d	Doubling time (days)	3.5 (3.0–4.0)	Estimated	—
Infectious disease transmission model parameters				
β	Transmission rate (1/day)	—	—	Estimated
σ	Latency rate (1/day)	—	—	(1/8, 1/4)
γ	Recovery rate (1/day)	—	—	(1/10, 1/5)
I_0	Infectious fraction at time 0	—	—	(1E-6, 1E-2)
κ	Size of the at-risk population	—	—	Estimated as $\kappa\varphi_{IC}$

Figure legends and alt text

Figure 1: *Anatomy of outbreak model projections and supporting data. A) On the current date, case data in the burn-in period (cross points) are incomplete because of reporting delays; they will eventually be filled in (open circles) but are not available on the current date (grey vertical line). The case data within the fitting period (black circles) inform the model projections (dotted line) and uncertainty region (grey ribbon) in the projection period. B) To incorporate data on reported cases, hospitalizations, and deaths and project them and infections, we need to account for both delays and ratios between them.*

Figure 1 alt text: *A two-panel figure. The first panel plots cases and a model fit with uncertainty bounds, with multiple annotations highlighting features of the data and model. The second panel plots reported and modeled cases, hospitalizations, and deaths and modeled infections, with annotated arrows highlighting the relationships between the data types.*

Figure 2: *A compartmental infectious disease model with susceptible (S), latent (L), infectious (I), and recovered (R) compartments. The model accounts for the transmission rate (β), the latency-to-infectiousness rate (σ), and the recovery rate (γ). To create realistic distributions of latent and infectious periods, the latent and infectious phases are each modeled as two consecutive compartments (distributed delay). This model can be expanded to account for mechanisms or data streams specific to the disease of interest.*

Figure 2 alt text: *A schematic of a compartmental infectious disease model, with arrows describing flows between compartments.*

Figure 3: Handling uncertainty for mechanistic infectious disease model forecasting. *We use a hybrid sampling–estimation approach to sample unidentifiable model parameters and estimate identifiable model parameters. A) We generate many combinations of reasonable values for the unidentifiable parameters. B) For each combination of unidentifiable parameters, we estimate the values of the identifiable parameters by maximizing the fit (minimizing the negative log-likelihood). C) We generate a projection for each combination of sampled and estimated parameters that reasonably fits the recent data. D) We display 50% and 95% credible intervals for the projected trajectories. This approach provides a full array of possible future trajectories consistent with the recent past.*

Figure 3 alt text: *A figure with four panels. A) A graph of sampled values of two parameters demonstrating coverage over the parameter space and a table of sets of sampled parameters.*

B) A graph of a negative log-likelihood indicating a maximum-likelihood best fit and a table of sets of estimated parameters. The tables of sampled and estimated parameters are connected by arrows indicating row-wise connections. C) A graph of case data and a large number of infectious disease trajectories that all fit the case data but have different projections. D) A graph of case data and two uncertainty regions.

Figure 4: Phase 1 (before local transmission) projections of A) reported cases, B) hospitalizations, and C) deaths*. The x-axis is days after a hypothetical first infection. The dotted lines represent best-guess projections, the lighter ribbons denote 95% credible intervals, and the darker ribbons denote 50% credible intervals.*

Figure 4 alt text: *A figure with three panels, each with a projected trajectory and ribbons denoting uncertainty regions.*

Figure 5: Phase 2 (local exponential growth) projections of A) reported cases, B) hospitalizations, and C) deaths*. The solid and dotted lines represent median projections in the data and projection periods, respectively, the lighter ribbons denote 95% confidence intervals, and the darker ribbons denote 50% confidence intervals. Case data are burned for 1 week prior to current date (November 1, 2020; vertical grey line) to account for reporting delays from symptom onset. Hospitalization and death data are delayed relative to cases, so we do not include data that do not correspond to the case data that inform the model fit (open points).*

Figure 5 alt text: *A figure with three panels, each with data and a projected trajectory and ribbons denoting uncertainty regions.*

Figure 6: Phase 3 (interventions and scenarios) projections of reported cases, hospitalizations, and deaths*. Status-quo projections are given in subfigures A–C, ±25% transmission rate scenarios in D–F, and 45% decreased transmission rate scenario, retrospectively compared to the eventually reported data in G–I. The lines represent median projections, the lighter ribbons denote 95% confidence intervals, and the darker ribbons denote 50% confidence intervals. Case data are burned for 1 week prior to current date (vertical grey line) to account for reporting delays. Hospitalization and death data are delayed relative to cases, so we do not include data (open points) that do not correspond to the case data that inform the model fit.*

Figure 6 alt text: *A figure with nine panels, each with data and a projected trajectory and ribbons denoting uncertainty regions.*

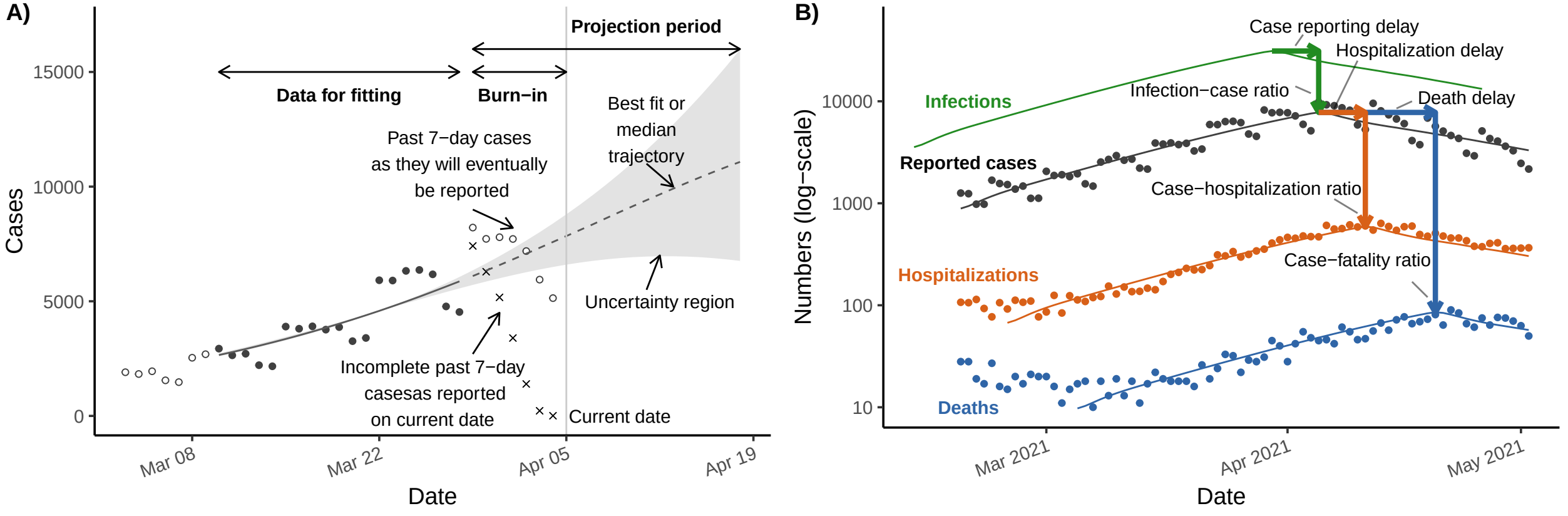
A)
Projection period
Data for fitting
Burn−in
Best fit or
median
trajectory
Past 7−day cases
as they will eventually
be reported
Uncertainty region
Incomplete past 7−day
casesas reported
on current date
Current date
Cases
15000
10000
5000
0
Mar 08
Mar 22
Apr 05
Apr 19
Date
B)
Case reporting delay
Hospitalization delay
Infection−case ratio
Death delay
Infections
Reported cases
Case−hospitalization ratio
Case−fatality ratio
Hospitalizations
Deaths
Numbers (log−scale)
10000
1000
100
10
Mar 2021
Apr 2021
May 2021
Date

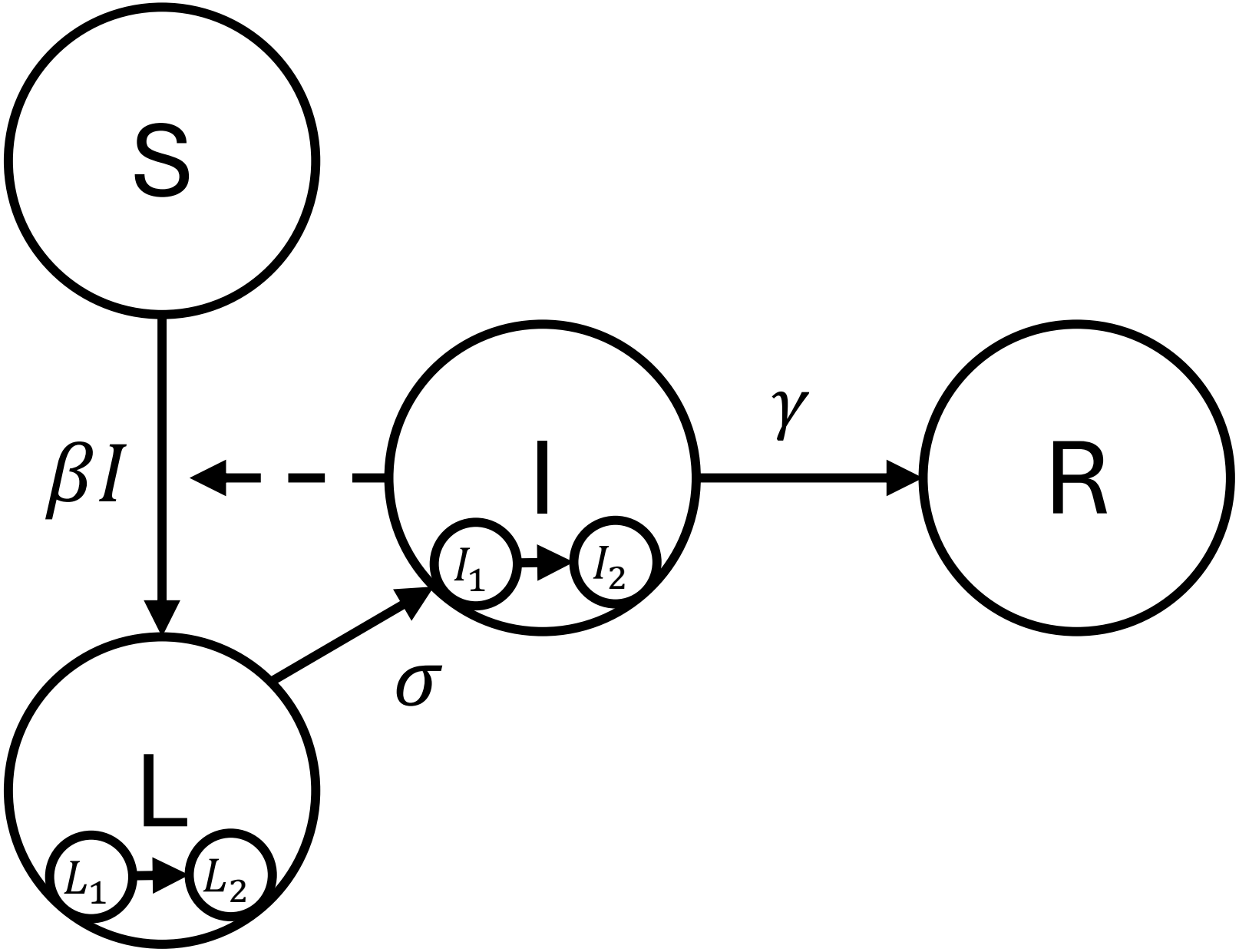
S
βI
I
I_1
I_2
γ
R
σ
L
L_1
L_2

A. Sample unidentifiable parameters across reasonable ranges

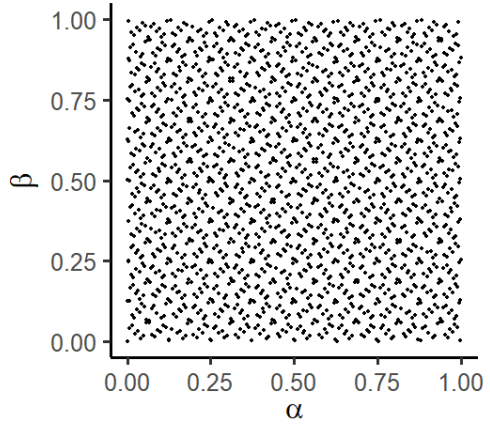

B. For each set of sampled parameters, estimate the best fit values of the identifiable parameters

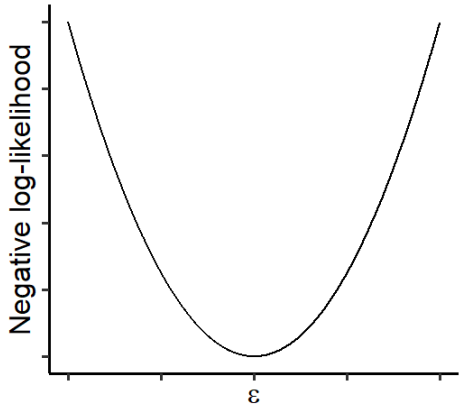

C. For set of sampled and estimated parameters, project the trajectory forward.

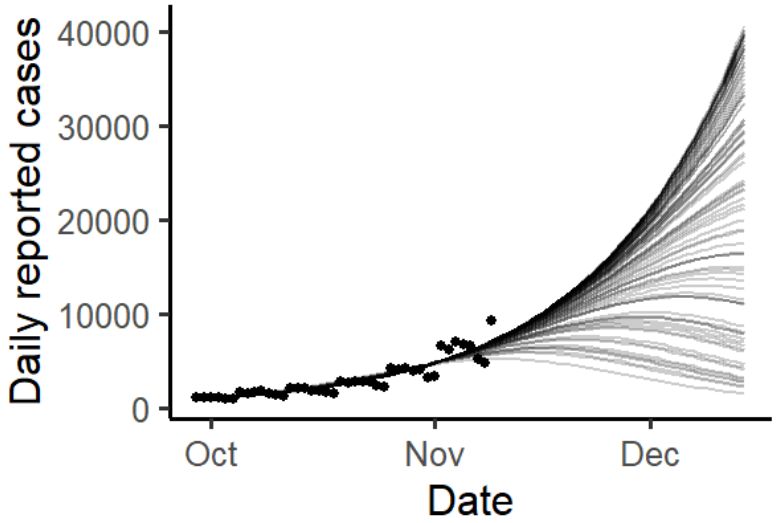

Sample	Parameter 1	Parameter 2	Parameter 3	Parameter 4
1	α_1	β_1	γ_1	δ_1
2	α_2	β_2	γ_2	δ_2
3	α_3	β_3	γ_3	δ_3
4	α_4	β_4	γ_4	δ_4
…				

	Parameter 5	Parameter 6
1	ε_1	ζ_1
2	ε_2	ζ_2
3	ε_3	ζ_3
4	ε_4	ζ_4
…		

D. Define pointwise credible intervals based on the set of trajectories.

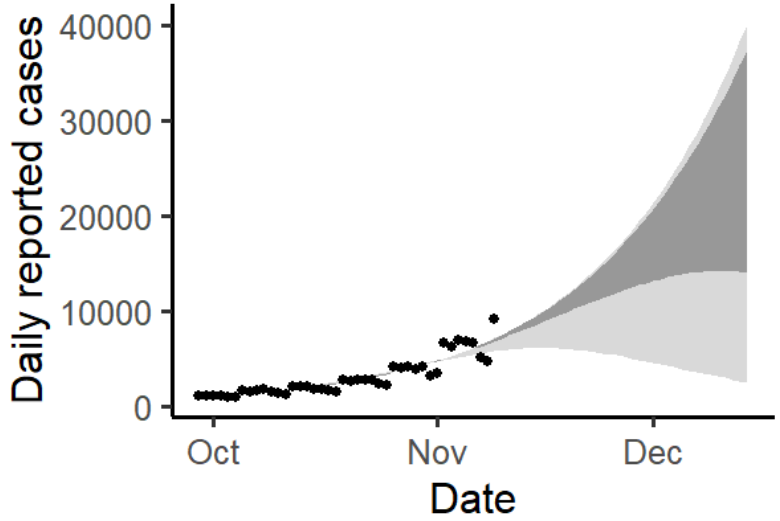

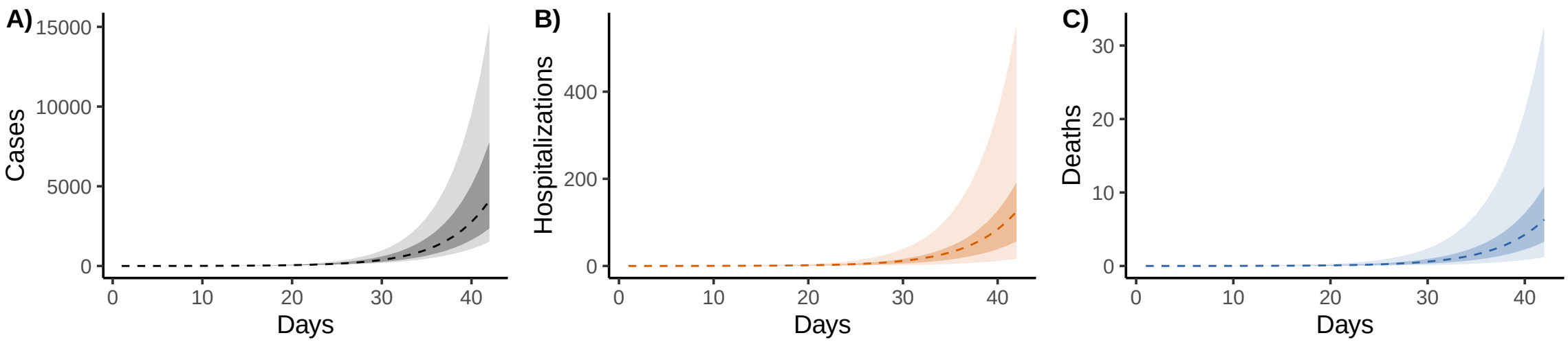
A)
Cases
15000
10000
5000
0
0
10
20
30
40
Days
B)
Hospitalizations
400
200
0
0
10
20
30
40
Days
C)
Deaths
30
20
10
0
0
10
20
30
40
Days

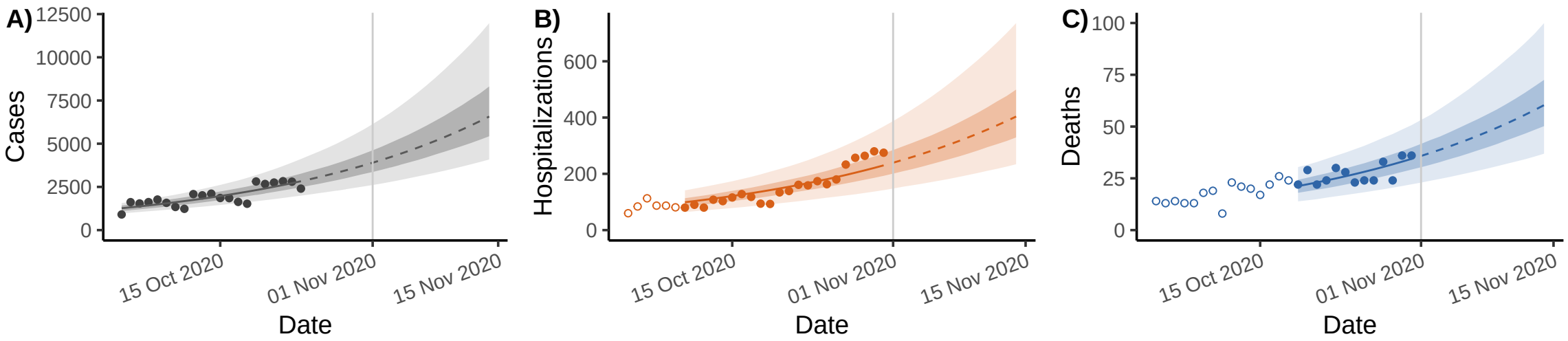
A)
Cases
12500
10000
7500
5000
2500
0
15 Oct 2020
01 Nov 2020
15 Nov 2020
Date
B)
Hospitalizations
600
400
200
0
15 Oct 2020
01 Nov 2020
15 Nov 2020
Date
C)
Deaths
100
75
50
25
0
15 Oct 2020
01 Nov 2020
15 Nov 2020
Date

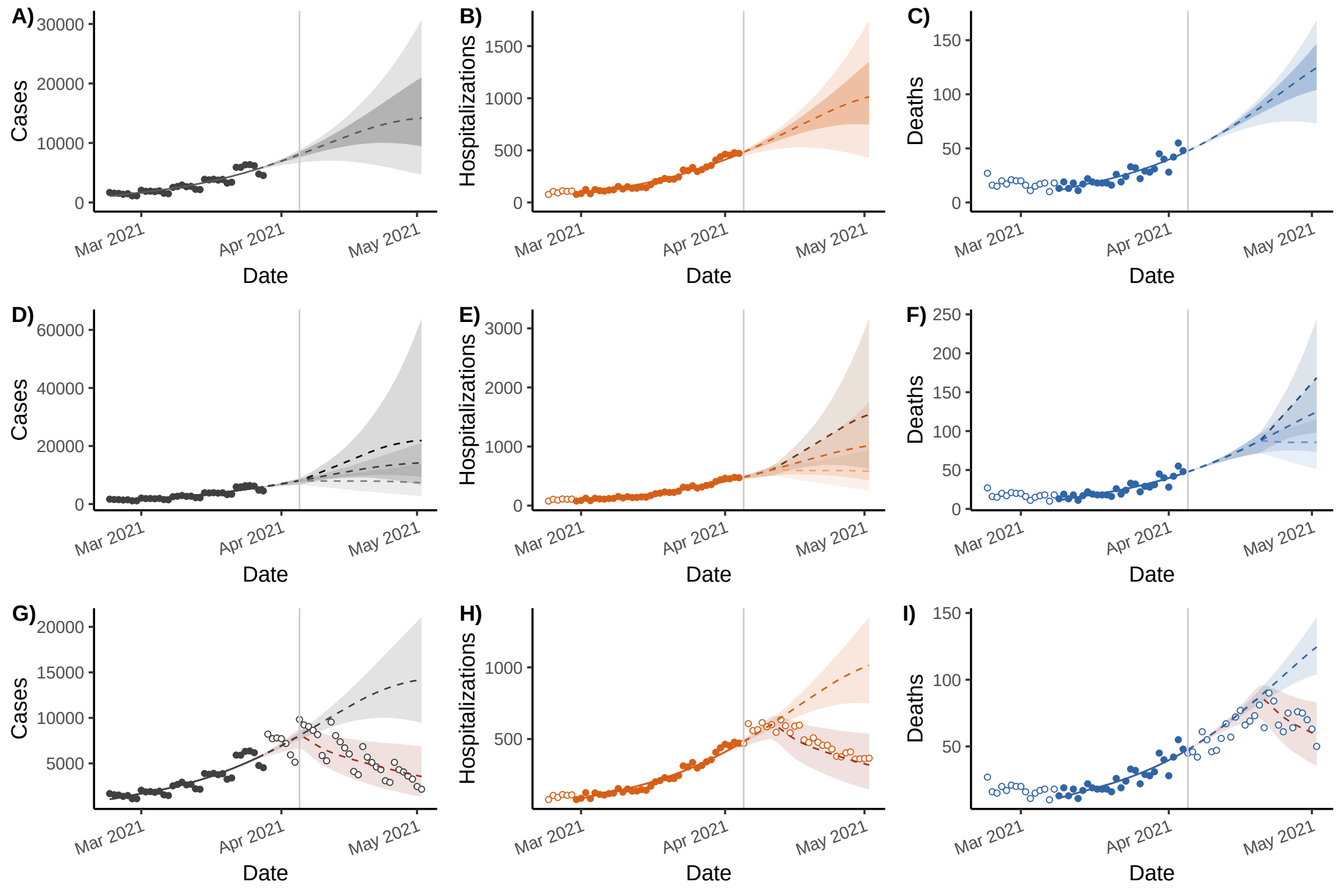
A)
Cases
30000
20000
10000
0
Mar 2021
Apr 2021
May 2021
Date
B)
Hospitalizations
1500
1000
500
0
Mar 2021
Apr 2021
May 2021
Date
C)
Deaths
150
100
50
0
Mar 2021
Apr 2021
May 2021
Date
D)
Cases
60000
40000
20000
0
Mar 2021
Apr 2021
May 2021
Date
E)
Hospitalizations
3000
2000
1000
0
Mar 2021
Apr 2021
May 2021
Date
F)
Deaths
250
200
150
100
50
0
Mar 2021
Apr 2021
May 2021
Date
G)
Cases
20000
15000
10000
5000
Mar 2021
Apr 2021
May 2021
Date
H)
Hospitalizations
1000
500
Mar 2021
Apr 2021
May 2021
Date
I)
Deaths
150
100
50
Mar 2021
Apr 2021
May 2021
Date